

### REMARKS

This Application has been carefully reviewed in light of the Final Office Action mailed September 7, 2005. At the time of the Final Office Action, Claims 1-7, 9-16 and 18 were pending in this Application. Claims 1-7, 9-16 and 18 were rejected. Claims 8 and 17 were previously cancelled without prejudice or disclaimer.

#### **Rejections under 35 U.S.C. §103**

Claims 1, 3, 7, 9, 10, 12, 16 and 18 were rejected under 35 U.S.C. §103(a) as being unpatentable over U.S. Patent No. 5,441,401 issued to Akira Yamaguro et al. ("Yamaguro") in view of European Patent Application Publication No. 537,968 by Yujiro Oshima et al. ("Oshima"), U.S. Patent No. 6,653,005 issued to Nazim Muradov ("Muradov") and the admitted prior art of Hornung et al. (p.8, line 31-p.9, line 5 of the instant application). Applicants respectfully traverse and submit the cited art combinations, even if proper, which Applicants do not concede, does not render the claimed embodiment of the invention obvious.

Amended Claims 1 and 10 are limited to a system operable in a diesel engine with a range of exhaust gas temperatures. As stated above, such engines have a wide range of exhaust gas temperatures, and can have very high exhaust gas temperature excursions.

The specification repeatedly states that the disclosed system and method are for use with diesel engines. For example, page 5, lines 10 - 11, states that "both embodiments are used with diesel engines....". Furthermore, it is clear that the diesel engines are vehicles. For example, page 8, line 15 refers to cold start operation. Page 9, line 24, refers to "tailpipe" oxides. Also, the Background makes clear that the invention is directed to vehicular diesel engine applications.

It cannot be disputed, and need not be explicitly stated, that the diesel engines that are the subject of the invention have a wide range of exhaust gas temperatures. The attached article from [www.fast-diesel.com](http://www.fast-diesel.com) is but one example of a discussion of diesel engine exhaust gas temperatures, and was easily found with a simple search engine query. As stated therein, exhaust gas temperatures can range from 150 degrees C at idle, to more than 700 degrees C under a high load. Under normal engine running conditions, exhaust gas temperatures range

from about 250 to 450 degrees C. These facts are so well known that they are without dispute.

Claims 7 and 16 have been cancelled and their recitations incorporated into Claims 1 and 10, respectively. Thus, Claims 1 and 10 are further limited to the use of ruthenium-based catalyst in a diesel automotive engine.

Claims 1 and 10 have been further amended to recite the use of a means for calculating the ratio of NO to NO<sub>2</sub>, and a metering device to maintain a ratio of hydrogen to NO. These features of the invention are recited on page 8, lines 16 - 30, and on page 15 - 18. Applicants will amend Figures 1 and 2 to include these features of the invention, if desired by the Examiner.

Applicants further wish to point out that Claims 1 and 10 explicitly recite the reduction of NO<sub>x</sub> emissions to nitrogen (N<sub>2</sub>), not some other nitrogen-containing compound such as NH<sub>3</sub> or NO<sub>2</sub>.

Applicants contend, as explained below, that the cited references do not make obvious the use of a ruthenium-based catalyst in an automotive diesel engine.

It is true that the article by Hornung discusses the use of ruthenium-based catalysts for selective reduction of NO by hydrogen. A copy of the Hornung article is attached to this response. For the Examiner's convenience, the attached Hornung article has been annotated with conversions from degrees Kelvin to degrees Celsius.

Hornung is silent with regard to applications for ruthenium-based catalysts. More significantly, Hornung teaches experimentation at low temperatures and in narrow operating ranges. For example, Figure 3b of Hornung teaches a very narrow, low temperature, reduction to nitrogen (N<sub>2</sub>). Specifically, significant nitrogen is shown as being produced only in a narrow range centered around 177 C. This narrow range and low temperature would not be suitable for use with vehicular diesel engines.

Furthermore, Hornung teaches the reduction of NO. However, it does not teach determining the relative levels of NO and NO<sub>2</sub> in automotive exhaust, and of determining a molar ratio of H<sub>2</sub> to NO<sub>x</sub> based on specified ratios of H<sub>2</sub> to NO and H<sub>2</sub> to NO<sub>2</sub>.

For these reasons, Claims 1 and 10 are allowable, as are their dependent claims.

**CONCLUSION**

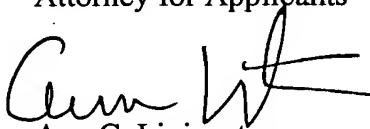
Applicants have made an earnest effort to place this case in condition for allowance in light of the amendments and remarks set forth above. Applicants respectfully request reconsideration of all pending claims.

Applicants enclose a Request for Continued Examination (RCE), and a check in the amount of \$395.00 for the RCE fee. Applicants also enclose a Petition for Three Month Extension of Time, and a check in the amount of \$510.00 for the extension fee. Applicants believe no additional fees are due at this time, however, the Commissioner is hereby authorized to charge any fees or credit any overpayments to Deposit Account No. 50-2148 of Baker Botts L.L.P. in order to effectuate this filing.

If there are any matters concerning this Application that may be cleared up in a telephone conversation, please contact Applicants' attorney at 512.322.2634.

Respectfully submitted,

BAKER BOTTS L.L.P.  
Attorney for Applicants

  
Ann C. Livingston  
Reg. No. 32,479

Date: January 25, 2006

SEND CORRESPONDENCE TO:

CUSTOMER ACCOUNT NO. **31625**

512.322.2634

512.322.8383 (fax)



## Home

## Company

## Products:

### GM/Chevy Duramax

#### 4" Aluminized Exhaust

#### Stainless Exhaust:

#### MBRP

#### Banks Monster

#### Programmers:

#### Superchips

#### Micro Tuner

#### Diablo Predator

#### On-Board Modules:

#### Edge Products

#### Edge A2

#### Banks Six-Gun

#### Six-Gun Bundles

#### Banks Power Kits

#### Back-Up Camera

#### Air Intake Systems:

#### aFe Magnum FORCE

#### AIRAID

#### TurboGuard

### Dodge Cummins

#### 5" Aluminized Exhaust

#### 4" Aluminized Exhaust

#### Stainless Exhaust:

#### MBRP

#### Banks Monster

#### Programmers:

## watching your egt's



Exhaust Gas Temperature (EGT) is a good indicator of your engine's performance. Accuracy in Exhaust Gas Temp (EGT) is very important. The turbo doesn't make heat; it absorbs the heat and uses the exhaust pressure. As the exhaust is blown across the turbine blades, the blades spin at incredible speeds. The shaft of the turbine wheel is slaved to the compressor wheel so they spin together. When you spool up the turbine, the compressor turns as well. Generally speaking, the faster it spins, the more boost the turbo will make. The problem comes when you're trying to spin the turbine too fast. To do this, it takes a lot of heat and pressure. If you get the turbine too hot, it can damage the turbo. At 1270° F, the tips of the turbine blades begin to glow. If you get them too hot, they'll straighten out or even melt and you'll ruin the turbo. Another danger is the heat causing excessive wear on the bushings. This will cause the compressor wheel to scrape the housing and take out the turbo all together.

There is contradictory opinion and advice about the best place to install the temperature reading device (thermocouple) that supports the pyrometer, but there is no disagreement that watching EGTs with a graduated gauge is a good thing to do.

EGT's will be different depending on the modifications done to the vehicle. This is a guide to use as a reference only. EGT's will run about 300° F at idle to 1400+° F under an extreme load (such as merging onto the interstate with 25,000 lbs.) Normal running temps will be between 500° to 900° F. So when you're out on the road, pay attention to the gauge. If EGT's start to creep up, simply ease out of the throttle.

Some publications dealing with EGT temps favor Turbocharger Inlet Temp (TIT) and not Turbocharger Outlet Temp (TOT). This suggests that the thermocouple should be mounted Pre-Turbo (in the exhaust manifold) and not Post-turbo. (in the down pipe) In their view, if you choose to mount the thermocouple in the down pipe, EGT readings will be inaccurate. With the thermocouple in the down pipe, the gauge reacts more slowly and is reading the TOT which is lower than the actual temp of the turbocharger. The difference between TIT and TOT can be as little as 50° F to as much as 400° F under a heavy load.

Other experts point out that installing the thermocouple in the exhaust manifold, ahead of the turbo, raises the possibility of the thermocouple breaking loose in the heated air stream and damaging the turbo. With greater accuracy goes greater risk.

One expert gauge manufacturer suggests that mounting the thermocouple in the downpipe and watching for a sustained temperature of 1050° F, is just as good as mounting in the pre-turbo position. Logic would suggest that if the temperature can

[Superchips](#)  
[Micro Tuner](#)  
[Superchips](#)  
[Flashpaq](#)

**On-Board Modules:**

[Edge Products](#)  
[Edge A2](#)  
[Banks Big Boss](#)  
[Banks Six-Gun](#)  
[Six-Gun Bundles](#)  
[Banks Power Kits](#)  
[Banks TechniCooler](#)  
**Air Intake Systems:**  
[aFe Magnum FORCE](#)  
[AIRAID](#)  
[Banks Ram-Air](#)  
**Exhaust Brakes:**  
[Banks Brake](#)  
[PacBrake](#)  
[Back-Up Camera](#)  
[Banks Billet](#)  
[Torque Converter](#)  
[TurboGuard](#)

**Hummer H2**

**Programmers:**

[Superchips](#)  
[Micro Tuner](#)  
[Diablo Predator](#)  
[Hypertech](#)

**Ford Powerstrokes**

**Find Heavy Equipment**

**Product Info**

[How Diesels Work](#)  
[How Turbos Work](#)  
[Banks Six-Gun](#)  
[Exhaust Gas Temp](#)  
[Know Your Gauges](#)  
[Magnusson Moss](#)  
[Edge Installation](#)  
[Banks Installation](#)

**Contact Us**

**Links**

vary as much as 400 degrees from the input to output side, then the sustained TOT temperature to be watched for under extreme load should be more like 870° F (1270° F "straightening" point minus the possible 400° F variation.)

The best location for installation of the thermocouple for a TOT application is in the downpipe as close to the turbo as possible. This article is based on our own research through the trade literature, and discussion with gauge manufacturers. You will generally find that neither the manufacturer of the truck, the engine, or the various manufacturers of pyrometers take a public position on where to put the thermocouple. Neither do we. In short, watching your EGT's is highly recommended if you operate under heavy load. And just as in deciding how fast to drive, there is risk and reward in deciding where to place the thermocouple. We hope that the information presented will help you to reach a reasoned conclusion on your own. If you need additional information, you should consult your Chevy or Dodge dealer.

[Return Policy](#) - [Privacy Policy](#) - [Important Disclaimers](#)



**Fast-Diesel.com**

200 Dale St.

Edgewater, FL 32132

Phone: 386.428.7080

Fax: 386.426.6298

Email: [info@fast-diesel.com](mailto:info@fast-diesel.com)

Do you like this site?  
 Your friends will too.  
[Click here to  
 recommend this site](#)



Submit your email  
 address to be notified  
 of new products and  
 features.

Edgewater Products, LLC dba [www.fast-diesel.com](http://www.fast-diesel.com) has no official relationship with the General Motors Corporation® or Daimler Benz® and nothing in this site should be construed as reflecting endorsement by these companies.



[Click to Verify](#)

© 2003-2004 Edgewater Products, LLC

Web Design and Hosting  
 by [Richard C. Church](#)

# On the mechanism of the selective catalytic reduction of NO to N<sub>2</sub> by H<sub>2</sub> over Ru/MgO and Ru/Al<sub>2</sub>O<sub>3</sub> catalysts

A. Hornung<sup>a</sup>, M. Muhler<sup>a,\*</sup> and G. Ertl<sup>b</sup>

<sup>a</sup> *Lehrstuhl für Technische Chemie, Ruhr-Universität Bochum, D-44780 Bochum, Germany*  
E-mail: muhler@techem.ruhr-uni-bochum.de

<sup>b</sup> *Fritz-Haber-Institut der Max-Planck-Gesellschaft, Faradayweg 4-6, D-14195 Berlin, Germany*

Steady-state and transient kinetic experiments were performed in a versatile microreactor flow set-up with magnesia- and alumina-supported ruthenium catalysts in order to elucidate the mechanism of the selective catalytic reduction (SCR) of nitric oxide with hydrogen. Both Ru/MgO and Ru/ $\gamma$ -Al<sub>2</sub>O<sub>3</sub> were found to be highly active catalysts converting NO and H<sub>2</sub> into N<sub>2</sub> and H<sub>2</sub>O with selectivities close to 100% at full conversion, although Ru-based catalysts are known to be active in the synthesis of NH<sub>3</sub> from N<sub>2</sub> and H<sub>2</sub>. Frontal chromatography experiments with NO at room temperature revealed that NO and its dissociation products displace adsorbed atomic hydrogen (H\*) almost completely from hydrogen-precovered Ru surfaces. Obviously, NO and H<sub>2</sub> compete for the same adsorption sites, H\* being the weaker bound adsorbate. Temperature-programmed surface reaction (TPSR) experiments in H<sub>2</sub> subsequent to NO exposure demonstrated that higher heating rates and lower partial pressures of H<sub>2</sub> shift the selectivity from NH<sub>3</sub> to N<sub>2</sub>. Therefore, the coverage of H\* is concluded to govern the branching ratio between the rate of associative desorption of N<sub>2</sub> (2N\* → N<sub>2</sub> + 2\*) and the rate of hydrogenation of N\* (N\* + 3H\* → NH<sub>3</sub> + 4\*). Finally, the steady-state coverages of N- and O-containing adsorbates were derived by interrupting the SCR reaction and hydrogenating the adsorbates off as NH<sub>3</sub> and H<sub>2</sub>O. By solving the site balance, the Ru surfaces were found to be essentially saturated by a N + O coadsorbate layer. Thus, the observed high steady-state SCR selectivity to N<sub>2</sub> is attributed to the very low coverage of H\* due to site blocking by a N + O coadsorbate layer, favouring the recombination of N\* instead of its hydrogenation to NH<sub>3</sub>.

**Keywords:** nitric oxide, selective catalytic reduction, supported ruthenium catalysts, frontal chromatography, temperature-programmed surface reaction, reaction mechanism

## 1. Introduction

Supported ruthenium catalysts are known to be very active in the selective catalytic reduction (SCR) of nitric oxides with hydrogen as well as with ammonia as a reductant (see, for example, [1,2] and references therein). The mainly interesting feature of these catalysts is their very high selectivity to nitrogen, contrary to other group VIII metals such as platinum. A detailed knowledge of the reaction mechanism on ruthenium is therefore of crucial importance for the tailored development of new SCR catalysts. While several studies were carried out to check the catalytic properties of Ru-based catalysts under different reaction conditions [3–8], to our knowledge, only few attempts were undertaken to unravel the reaction mechanism [9–11]. All the catalysts investigated in these studies were prepared using RuCl<sub>3</sub> as metal precursor, due to its low cost and easy availability. Since adsorbed atomic chlorine can lead to severe changes of the catalyst activity and selectivity due to selective poisoning of the surface sites responsible for the dissociative adsorption of H<sub>2</sub>, its absence is mandatory for the assessment of the reaction mechanism. In a previous study, first results of a systematic transient kinetic study of the reduction of NO with H<sub>2</sub> on a Cl-free, magnesia-supported ruthenium catalyst were presented [2]. It was suggested that the observed high selectivity to N<sub>2</sub> in the

steady-state reaction was correlated with a high coverage of the surface with nitrogen- and oxygen-containing adsorbates, keeping the coverage of adsorbed atomic hydrogen (H\*) low and thus suppressing the formation of NH<sub>3</sub>. This conclusion was derived from frontal chromatography experiments with NO followed by temperature-programmed desorption (TPD) and temperature-programmed surface reaction (TPSR) experiments.

The frontal chromatographic adsorption of nitric oxide at room temperature was found to be accompanied by the desorption of molecular nitrogen, clearly indicating that at least 20% of the adsorbed NO dissociates at room temperature, presumably before reaching saturation [2]. On the other hand, former investigations [12,13] with Ru/MgO catalysts showed that no desorption of nitrogen takes place at room temperature after saturation of the surface with adsorbed atomic nitrogen (N\*) by exposure to N<sub>2</sub>, in analogy with studies on the Ru(0001) single-crystal surface under ultrahigh-vacuum conditions [14,15], which clearly showed that exposing this surface to N<sub>2</sub> leads to the formation of a stable N-2×2 adsorbate structure (N<sub>2</sub>) with a maximum surface coverage of 0.25 characterised by a high desorption temperature. A higher coverage of 0.33 was, however, reached by decomposition of NH<sub>3</sub>, characterised by a closer packing into domains of a  $\sqrt{3} \times \sqrt{3} R30^\circ$ -phase (N<sub>3</sub>) with a considerably lower adsorption energy, leading to a low-temperature peak in the thermal desorption spectrum. Our previous TPD results showed that the disso-

\* To whom correspondence should be addressed.

ciative chemisorption of nitric oxide also leads to the population of the  $N_\beta$ -state, an effect which is prompted by the simultaneously formed adsorbed O atoms which also occupy hcp sites [2]. Scanning tunnelling microscopy (STM) investigations of the adsorption of NO on the Ru(0001) single-crystal surface at room temperature revealed that, at higher coverage, coadsorbed N and O atoms form mixed phases with an approximately random occupation of the adsorption sites [16]. Thus, it can be safely concluded that the presence of adsorbed oxygen atoms (O\*) has a similar effect on the energetics of nitrogen chemisorption as higher coverages of N\*.

It is well known that ruthenium-based catalysts are highly active in the synthesis of  $NH_3$  from  $N_2$  and  $H_2$  through the hydrogenation of N\* by H\* [17,18]. It was speculated that the low  $NH_3$  slip in the SCR process over Ru-based catalysts was due to the high activity of these catalysts in the synthesis and, consequently, also in the decomposition of  $NH_3$  [5–7], but the origin of the high selectivity to  $N_2$  as a product of the reduction of NO with  $H_2$  remained essentially unclear. Furthermore, previous studies of ammonia synthesis over magnesia- and alumina-supported Ru-based catalysts (see, for example, [18] and references therein) showed that the different support materials strongly affect the  $NH_3$  yield, the MgO-supported catalyst being the most active towards the production of  $NH_3$ . The kinetics of the surface processes were studied in the present work both on high-purity MgO- and  $\gamma$ - $Al_2O_3$ -supported Ru catalysts by means of stationary as well as transient methods comprising NO frontal chromatography, TPSR experiments with various heating rates and partial pressures of  $H_2$ , and titration experiments subsequent to quenching the steady-state SCR reaction.

## 2. Experimental

### 2.1. Catalyst preparation and characterisation

The catalysts were prepared by wet impregnation, as described in [19], in order to achieve a metal loading of about 5 wt% Ru. The same procedure was followed for the preparation of both Ru/MgO and Ru/ $\gamma$ - $Al_2O_3$ . As support materials, MgO (Puratronic, 99.9955% metals basis, Johnson Matthey) and  $\gamma$ - $Al_2O_3$  (99.99%, Johnson Matthey) were chosen. The support material was heated in high vacuum at 773 K for 6 h and then dispersed in a solution of  $Ru_3(CO)_{12}$  (Johnson Matthey, 99%) in  $THF_{abs}$  for 4 h at room temperature. The impregnation step was carried out under inert gas atmosphere in a rotary evaporator to avoid contact with air and moisture. After evaporating the solvent at 313 K, the powder was pressed at a pressure of ca. 25 MPa into cylindrical pellets, which were subsequently crushed and sieved. The 250–450  $\mu m$  sieve fraction was slowly heated in high vacuum up to 723 K to decompose the adsorbed ruthenium complex. The Ru metal area

was determined by volumetric  $H_2$  chemisorption at room temperature in the quartz U-tube of an Autosorb 1-C set-up (Quantachrome) following the procedure described in [20]. Prior to chemisorption, the catalysts were reduced by high-purity ammonia synthesis gas (mass flow: 80 Nml min<sup>-1</sup>,  $H_2:N_2 = 3:1$ ) heating up to 773 K with a linear heating rate of 1 K min<sup>-1</sup>. The volume fraction of  $NH_3$  in the effluent gas was analysed at steady-state by a non-dispersive infrared detector (BINOS, Fisher–Rosemount) to determine the catalytic activity and compare the new catalyst to former charges. The total surface area was measured by static  $N_2$  physisorption (BET method) in the same set-up.

### 2.2. Steady-state and transient kinetic experiments

The steady-state measurements were carried out in an all stainless-steel flow system described in detail in [2]. It was equipped with a calibrated mass spectrometer (BALZERS, QMS 125) and a combined non-dispersive IR and UV detector (BINOS, Fisher–Rosemount) for the quantitative analysis of NO and  $NO_2$ , respectively. The reactor consisted of a quartz U-tube with an inner diameter of 3.9 mm, heated by a cylindrical aluminium oven. The amount of catalyst employed for all experiments was 0.200 g of the 250–450  $\mu m$  sieve fraction, resulting in bed heights of ca. 17 mm, which ascertained the absence of limitations by heat or mass transport. The steady-state investigations were carried out using a gas mixture containing 900 ppm of NO and 3%  $H_2$  in Ar at a constant total flow of 120 Nml min<sup>-1</sup>, corresponding to a GHSV of about 35000 h<sup>-1</sup>.

The stainless-steel set-up for the transient experiments was described in detail in [21]. This set-up was additionally equipped with a self-constructed gas-mixing station, which allowed the preparation of high-purity gas mixtures of the desired composition. A stainless-steel glass-lined U-tube having an inner diameter of 3.9 mm was used as reactor. A calibrated mass spectrometer (BALZERS, GAM 445) allowed a fast and quantitative online analysis of the gas-phase composition at the reactor outlet. Before each experiment, the catalyst was heated at 773 K for at least 2 h in flowing He (99.9999%, Linde; 50 Nml min<sup>-1</sup>) in order to achieve an adsorbate-free surface. The adsorption of NO was carried out by frontal chromatography at room temperature onto the adsorbate-free catalyst surface with a flow of 40 Nml min<sup>-1</sup> of NO diluted in He (2610 ppm NO, 99.9999%, Linde). The procedure was monitored by means of the mass spectrometer and interrupted after the breakthrough of the NO concentration front. The hydrogenation of the surface species formed after saturation with NO at room temperature was investigated by TPSR with  $H_2$  (99.9999%, Linde; 50 Nml min<sup>-1</sup>), whereby heating rates as well as the partial pressure of  $H_2$  in the gas phase were varied.

### 3. Results and discussion

#### 3.1. Catalyst characterisation and steady-state SCR results

The results of the N<sub>2</sub> physisorption and H<sub>2</sub> chemisorption measurements are summarised in table 1.

These data show that it was possible to synthesise two Ru catalysts with different supports, but only slightly differing specific metal surface areas and metal particle sizes, which makes them highly suitable for the investigation of support effects on the catalytic properties. Both catalysts showed the expected activity and high selectivity to nitrogen at low temperatures, reaching 100% conversion at temperatures as low as 450 K in the case of Ru/MgO and 470 K in the case of Ru/Al<sub>2</sub>O<sub>3</sub>. The maximum observed selectivity to N<sub>2</sub> was of 98.8% in the case of Ru/MgO, and the only other detectable N-containing species at 100% conversion was NH<sub>3</sub>. The formation of N<sub>2</sub>O was detected for both systems only at low conversion temperatures, with a maximum at conversions between 10 and 20%. These observations suggest that two reactions occur concurrently, which are controlled by the kind and amount of adsorbates on the catalyst surface. One can assume that at low temperatures the metal surface is covered almost to saturation with

molecularly adsorbed NO and its dissociation products, so that the formation of N<sub>2</sub>O is favoured by the reaction of N-\* with NO-\*. Increasing the temperature enhances the rate of the associative desorption of N<sub>2</sub>, the reaction rate of O-\* with H-\* forming H<sub>2</sub>O, and the rate of NO dissociation, thus suppressing the formation of N<sub>2</sub>O. No particular effect of the supporting material on activity and/or selectivity was observed, in contrast to the findings in the case of NH<sub>3</sub> synthesis.

#### 3.2. The adsorption of nitric oxide at room temperature

Under steady-state SCR conditions, the adsorbates NO-\*, N-\*, O-\* and H-\* compete for the empty Ru surface sites. O-\* is known to be the most strongly bound adsorbate, which can only be desorbed at temperatures above 1000 K. The relative stability of the adsorbates is reflected by NO frontal chromatography experiments with Ru/MgO. Figure 1(a) shows the gas-phase concentrations in the reactor effluent as a function of time. As mentioned in section 1, the formation of N<sub>2</sub> is observed prior to the breakthrough of the NO front. The quantitative results are summarised in table 2. The experiment was repeated with hydrogen-precovered Ru/MgO obtained by dosing H<sub>2</sub> at room temperature for 1 h over the initially adsorbate-free catalyst. Figure 1(b) shows that H-\* is displaced as H<sub>2</sub> during the experiment. A subsequently performed TPD experiment in He following dosing NO on the hydrogen-precovered catalyst revealed the desorption of only 7 μmol/g H<sub>2</sub> in addition to the N-containing species. Thus, the displacement of H-\* by NO and its dissociation products is almost complete, indicating clearly that NO and H<sub>2</sub> compete for the same adsorption sites, and that H-\* is the more weakly bound adsorbate.

Table 1  
Characterisation of Ru/MgO and Ru/Al<sub>2</sub>O<sub>3</sub>.<sup>a</sup>

	Catalyst	
	Ru/MgO	Ru/γ-Al <sub>2</sub> O <sub>3</sub>
BET area (m <sup>2</sup> g <sup>-1</sup> )	25.0	104.4
Surface Ru atoms (μmol g <sup>-1</sup> )	206	236
Specific metal surface areas (m <sup>2</sup> g <sup>-1</sup> )	10.3	11.7
Dispersion (%)	42	48
Metal particle size (nm)	2.4	2.1

<sup>a</sup> The Ru metal surface area was measured by means of static H<sub>2</sub> chemisorption at room temperature and calculated assuming a H:Ru ratio of 1:1 [19].

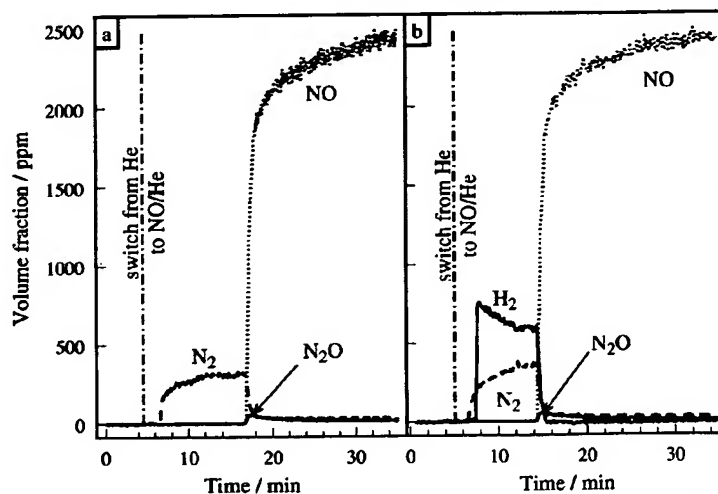


Figure 1. Frontal chromatography experiments with NO at room temperature with Ru/MgO after removal of all adsorbed species by heating in He up to 773 K (a), and after exposure to flowing H<sub>2</sub> at room temperature for 1 h (b).



Table 2  
Quantitative results of the NO frontal chromatography experiments with Ru/MgO at room temperature.

	Pretreatment	
	2 h in He at 773 K <sup>a</sup>	2 h in He at 773 K, followed by 1 h in H <sub>2</sub> at 300 K <sup>b</sup>
Adsorbed NO ( $\mu\text{mol g}^{-1}$ )	264	205
Desorbed H <sub>2</sub> ( $\mu\text{mol g}^{-1}$ )	—	40
Desorbed N <sub>2</sub> ( $\mu\text{mol g}^{-1}$ )	28	26
Desorbed N <sub>2</sub> O ( $\mu\text{mol g}^{-1}$ )	4	3

<sup>a</sup> Figure 1(a).

<sup>b</sup> Figure 1(b).

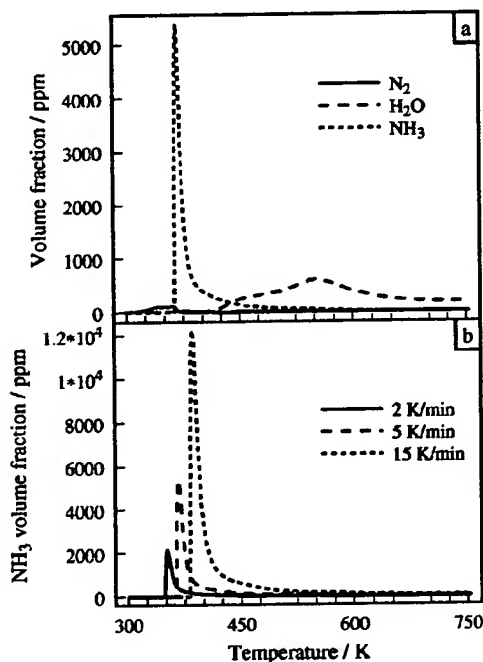


Figure 2. Temperature-programmed surface reaction data for Ru/MgO measured with a flow of 50 Nml min<sup>-1</sup> H<sub>2</sub> after saturating with NO at room temperature. (a) Heating rate 5 K min<sup>-1</sup> and (b) effect of the variation of the heating rate on the formation of NH<sub>3</sub>.

### 3.3. TPSR of nitric oxide with hydrogen

The results of the TPSR experiments in flowing H<sub>2</sub> with the NO-saturated Ru/MgO catalyst are depicted in figure 2. Both catalysts showed again qualitatively identical behaviour, the main differences being that the NH<sub>3</sub> peaks from the Al<sub>2</sub>O<sub>3</sub>-supported system were shifted to higher temperatures by 20 K and broadened because of the strong interaction of NH<sub>3</sub> with the acidic support, and the formation of a very small amount (5–6 ppm) of N<sub>2</sub>O in the temperature range between 300 and 400 K. Figure 2(a) shows the evolution of all observed species (N<sub>2</sub>, NH<sub>3</sub> and H<sub>2</sub>O) in the experiment with a heating rate of 5 K min<sup>-1</sup>. The main N-containing product was NH<sub>3</sub>, which was formed by an autocatalytic mechanism at a temperature of 360 K,

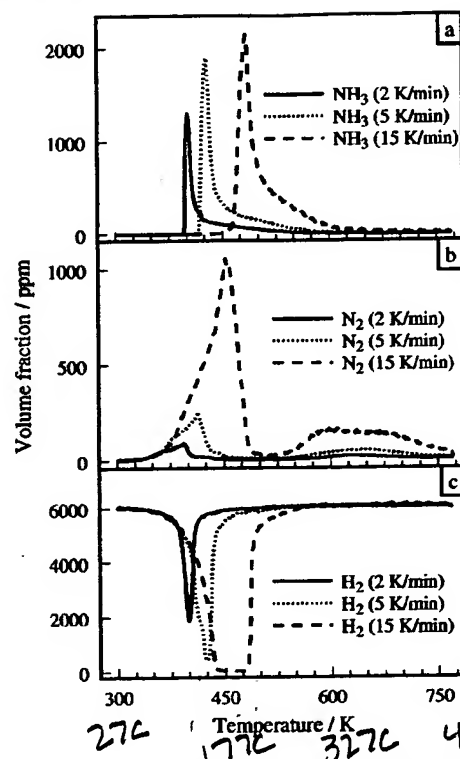


Figure 3. Temperature-programmed surface reaction data for Ru/MgO obtained with 50 Nml min<sup>-1</sup> H<sub>2</sub>/He (0.6 vol%) and three different heating rates of 2, 5 and 15 K min<sup>-1</sup> after saturating with NO at room temperature: (a) NH<sub>3</sub> formation, (b) N<sub>2</sub> desorption and (c) H<sub>2</sub> consumption.

preceded by the desorption of a small amount of N<sub>2</sub> [2]. A quantitative analysis of the experimental data showed that the selectivity to NH<sub>3</sub>, contrary to the steady-state results, was 92%. The formation of H<sub>2</sub>O started at a temperature of 400 K, after almost all N-containing species had desorbed from the Ru surfaces. The large width of the H<sub>2</sub>O peak is due to the strong interaction of H<sub>2</sub>O with MgO used as support. Figure 2(b) illustrates the effect of the variation of the heating rate on the onset and the peak maximum of the NH<sub>3</sub> formation: with increasing heating rate both the onset temperature and the peak maximum are shifting towards higher temperatures. A similar observation was made previously in TPSR experiments with the same catalyst after dosing molecular nitrogen to saturation [22]. However, in that case the formation of NH<sub>3</sub> was not preceded by N<sub>2</sub> desorption and the NH<sub>3</sub> peak was broader. These differences confirm our hypothesis that N-\* becomes thermally destabilized by high initial coverages of both N-\* and O-\*. The variation in selectivity of the transient and the steady-state reaction experiments suggests that the N<sub>2</sub>:NH<sub>3</sub> branching ratio is affected by the relative surface coverages of the species involved. In order to check this suggestion, a series of TPSR experiments with diluted H<sub>2</sub> (0.6 vol% in He) was performed with three different heating rates (2, 5 and 15 K min<sup>-1</sup>). The results are shown in figure 3: again the autocatalytic formation of NH<sub>3</sub> was observed, whereas,

NH<sub>3</sub>  
is  
ammonia

NO<sub>2</sub> nitrogen  
dioxide  
→ smog  
acid rain

876

Table 3  
Selectivity towards the formation of N<sub>2</sub> and NH<sub>3</sub> as a function of the heating rate of the TPSR experiment with 0.6 vol% H<sub>2</sub> in He.

	Heating rate (K min <sup>-1</sup> )		
	2	5	15
Selectivity (%)			
N <sub>2</sub>	40.1	46.2	68.6
NH <sub>3</sub>	59.9	53.8	31.4

as expected, the fraction of N-\* being converted into N<sub>2</sub> increased with increasing heating rate. Moreover, higher heating rates lead to a dramatic change in the N<sub>2</sub>:NH<sub>3</sub> branching ratio in favour of the formation of N<sub>2</sub>. The selectivity data are summarised in table 3. A closer inspection of figure 3(c) reveals the origin of the high selectivity to N<sub>2</sub> at a heating rate of 15 K min<sup>-1</sup>. Due to the reduced time-scale of the TPSR experiment, the H<sub>2</sub> uptake peak is shifted to higher temperatures, leading to the complete consumption of gas-phase H<sub>2</sub> in the temperature range from about 440 to 480 K. During this period of time essentially only the desorption of N<sub>2</sub> is taking place with increasing rates, while the formation of NH<sub>3</sub> suddenly sets in only at about 480 K.

Figure 4 summarises the quantitative results of a systematic series of TPSR experiments with different H<sub>2</sub> partial pressures in the gas phase over Ru/Al<sub>2</sub>O<sub>3</sub>. These results confirm the TPSR results obtained with Ru/MgO. A strong dependence of the selectivity on the coverage of H-\* is observed, with lower pressures of H<sub>2</sub> clearly favouring the formation of N<sub>2</sub>.

### 3.4. Determination of the surface coverages under SCR conditions at steady state

The quantification of the coverages of the N- and O-containing surface species under steady-state reaction conditions was carried out in the set-up for transient experi-

ments as follows: first a gas mixture containing 800 ppm NO and 2.6 vol% H<sub>2</sub> in He was passed over the catalyst at constant temperature with a flow of 50 Nml min<sup>-1</sup> (GHSV = 15000 h<sup>-1</sup>) until steady state was reached. At this point the gas flow was switched to pure H<sub>2</sub> (50 Nml min<sup>-1</sup>) at constant temperature in order to remove all N-containing adsorbed species in form of NH<sub>3</sub>. The integration of the NH<sub>3</sub> signal yields the nitrogen coverage. A subsequent TPSR experiment in H<sub>2</sub> was carried out to ensure the complete hydrogenation of all N-containing adsorbates. The determination of the oxygen coverage was less straightforward, due to the problem of accumulation of H<sub>2</sub>O on MgO during the reaction. After reaching steady-state reaction conditions, as described above, the flowing gas was switched at reaction temperature to pure He in order to quench the reaction. After having waited for all the signals to reach zero concentration, a TPD experiment was carried out to ensure the complete desorption of H<sub>2</sub>O from the support. Since in the chosen temperature range the desorption of O<sub>2</sub> from Ru cannot take place, the only way to remove O-\* is to hydrogenate it to H<sub>2</sub>O. After completion of the TPD experiment at a temperature of 773 K, the gas flow was switched to pure H<sub>2</sub> (50 Nml min<sup>-1</sup>) and the resulting sharp H<sub>2</sub>O signal was integrated to determine the amount of oxygen present on the surface. The whole procedure was repeated for the following reaction temperatures: 390, 410, 430 and 450 K.

Figure 5 shows a typical experimental sequence for the quantitative determination of the coverage of all N-containing adsorbates on Ru/MgO. Figure 5(a) shows the switching of the gas-phase composition from the SCR feed to pure H<sub>2</sub>, the subsequent TPSR experiment in H<sub>2</sub> is depicted in figure 5(b). The experimental procedure for the measurement of the coverage of O-containing adsorbates is illustrated in figure 6: (a) shows the interruption of the steady-state reaction by switching to pure He, (b) the subsequent TPD in He with a broad H<sub>2</sub>O desorption peak from

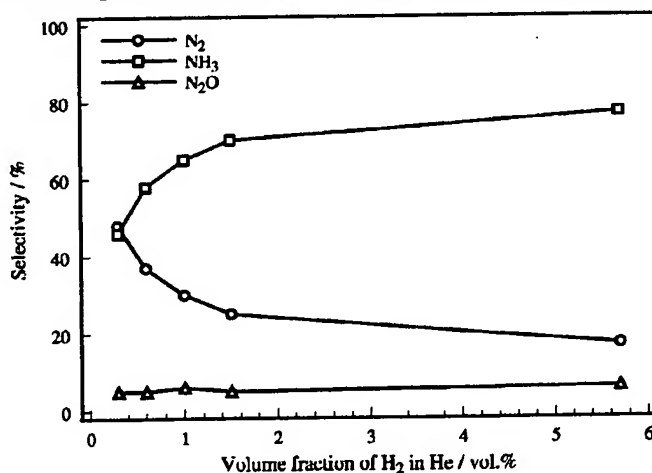


Figure 4. Selectivity data of temperature-programmed surface reaction experiments for Ru/ $\gamma$ -Al<sub>2</sub>O<sub>3</sub> after saturating with NO at room temperature as a function of the partial pressure of H<sub>2</sub> in the gas phase. Gas flow 50 Nml min<sup>-1</sup> H<sub>2</sub>/He, heating rate 5 K min<sup>-1</sup>.

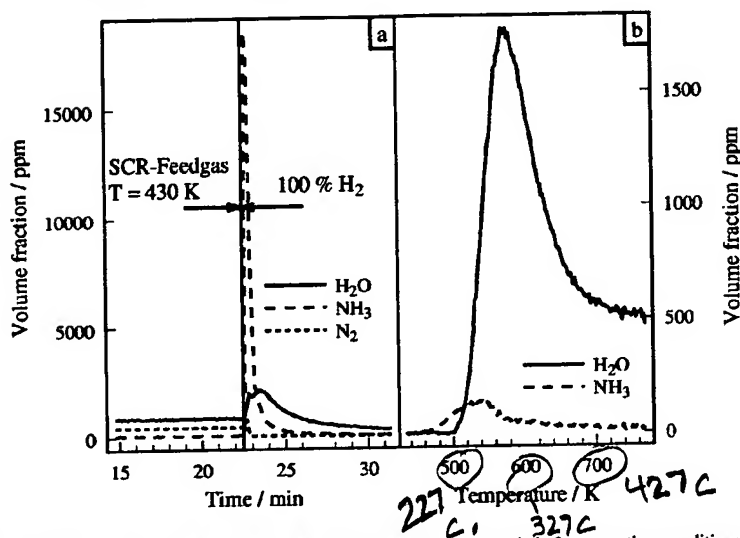


Figure 5. Determination of the coverage of N\* on Ru/MgO under SCR conditions. (a) Switch from reaction conditions to pure H<sub>2</sub> (50 Nml min<sup>-1</sup>) and (b) subsequent TPSR in H<sub>2</sub> (heating rate 5 K min<sup>-1</sup>).

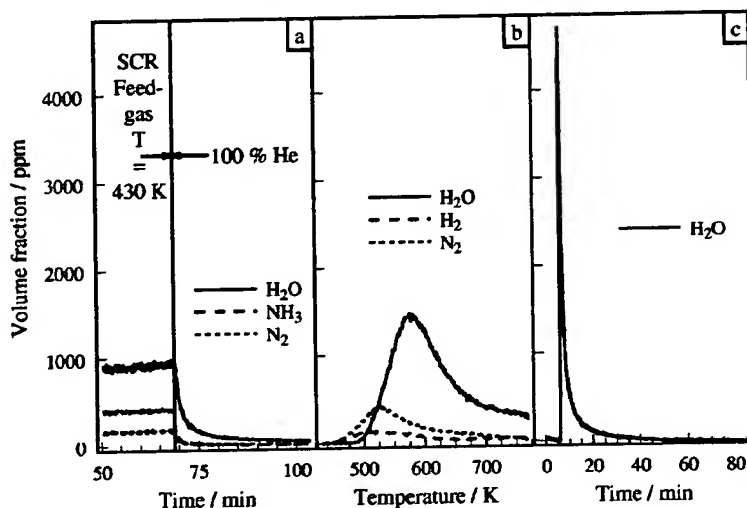


Figure 6. Determination of the coverage of O\* on Ru/MgO under SCR conditions. (a) Switch from reaction conditions to pure He (50 Nml min<sup>-1</sup>), (b) subsequent TPD in He (heating rate 5 K min<sup>-1</sup>) and (c) switch from He to pure H<sub>2</sub> at 773 K (50 Nml min<sup>-1</sup>).

the support. Finally, in figure 6(c) the switch to pure H<sub>2</sub> after completion of the TPD experiment is depicted. The quantitative results for the coverage values at the four reaction temperatures studied are summarised in table 4. These data confirm that, under steady-state reaction conditions at full NO conversion the catalyst surface is completely covered with nitrogen- and oxygen-containing species in a ratio of about 1 : 1. However, no statement about the precise nature of the adsorbates can be made alone on the basis of these investigations, since the experiments do not allow to distinguish between, e.g., N\* and NH\* or O\* and OH\*. The observation that the sum of the coverages at a reaction temperature of 390 K is greater than one points to the additional presence of molecularly adsorbed NO.

Table 4  
Nitrogen and oxygen coverages as a function of the temperature of the steady-state catalytic reduction of 800 ppm NO with 2.6 vol% H<sub>2</sub> in He.

	Temperature (K)			
	390	410	430	450
Coverage (%)				
N-containing adsorbates	0.68	0.46	0.49	0.47
O-containing adsorbates	0.67	0.49	0.46	0.48

### 3.5. Reaction mechanism

The steady-state and transient kinetic results can be rationalised in the catalytic cycle shown in figure 7. At temperatures below 393 K, the surface will be mainly covered by O\* and NO\*, and the few N atoms created by NO

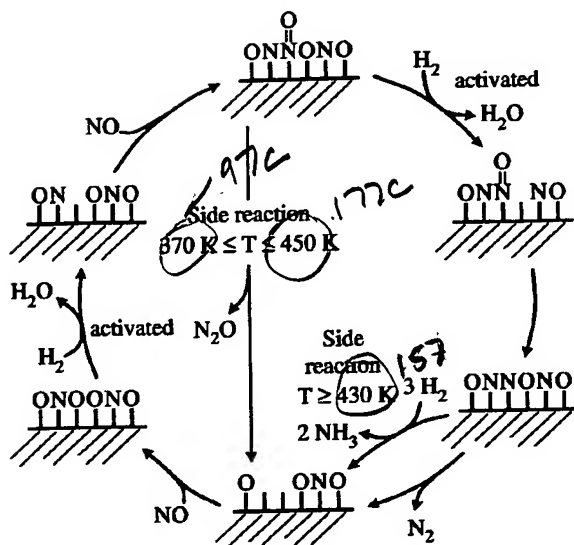


Figure 7. Proposed catalytic cycle for the selective catalytic reduction of NO with  $H_2$  over supported Ru catalysts.

dissociation react preferentially with NO to  $N_2O$ . At higher temperatures, the increasing conversion of  $O^*$  into  $H_2O$  will create free surface sites for the dissociation of NO, progressively suppressing the reaction path to  $N_2O$  in favour of the formation of  $N_2$  and  $NH_3$ . The recombination of two  $N^*$  to  $N_2$  dominates under these conditions over  $NH_3$  formation, since  $H_2$  and NO compete for free adsorption sites, whereby  $N^*$  and  $O^*$  are considerably stronger bound to the surface than  $H^*$ . As long as sufficient NO is present in the gas phase, the coverage of  $H^*$ , and hence the  $NH_3$  yield, will be low.

Finally, the question about the rate-determining step has to be discussed. The dissociation of NO on Ru(0001) was found to occur at 300 K predominantly at steps with high rates [23]. Correspondingly, the formation of  $N_2$  was observed at room temperature during the NO frontal chromatography experiment, clearly indicating dissociative adsorption on the supported Ru catalysts. On the other hand, the TPSR experiments showed that the hydrogenation of the  $N+O$  coadsorbate layer is a thermally activated process occurring in the temperature range of the onset of the steady-state SCR reaction. Thus, it seems safe to conclude that the rate-determining step of the overall reaction is the hydrogenation of  $O^*$  to  $H_2O$ , creating new free surface sites for the further dissociation of nitric oxide and determining the minimum temperature required for the full conversion of NO. A similar mechanism was proposed by Burch et al. [24] for the SCR reaction in the presence of excess  $O_2$  on oxide-supported Pt catalysts. The proposed mechanism also helps to rationalise why no significant influence of the support on the catalytic properties was found. Since MgO can act as electronic promoter only under highly reducing conditions, this effect is absent under SCR reaction conditions. Thus, the only role of the support is to sta-

bilise the high Ru dispersion, with roughly equal Ru metal surface areas leading to roughly the same catalytic activity. However, promoters which enhance the rate of  $O^*$  hydrogenation should lead to a higher catalytic activity.

#### 4. Conclusions

Two different supported Ru catalysts with comparable metal surface area and particle size were prepared, and their reactivity in the selective catalytic reduction of nitric oxide was investigated. Both the MgO- and the  $\gamma-Al_2O_3$ -supported catalysts were found to be highly active for the reduction of NO with  $H_2$  to  $N_2$ . Frontal chromatography experiments with NO over hydrogen-precovered Ru/MgO demonstrated that  $H^*$  is the more weakly bound adsorbate, and that NO and  $H_2$  compete for the same adsorption sites. TPSR experiments with varying heating rates and partial pressures of  $H_2$  revealed that  $H^*$  determines the branching ratio between the formation of  $N_2$  and  $NH_3$ . The Ru surfaces were found to be saturated with a  $N+O$  coadsorbate layer under steady-state SCR conditions suppressing the adsorption of  $H_2$  and thus the formation of  $NH_3$ . Furthermore, the high coverages of N- and O-containing adsorbates lead to destabilisation of chemisorbed N-atoms and hence to an enhanced rate of  $N_2$  desorption. As a consequence, high selectivities with respect to  $N_2$  formation by recombination of  $N^*$  are achieved under steady-state reaction conditions.

#### References

- [1] H. Bosch and F. Janssen, *Catal. Today* 2 (1988) 369.
- [2] A. Hornung, M. Muhler and G. Ertl, *Catal. Lett.* 53 (1998) 77.
- [3] M. Shelef and H.S. Gandhi, *Ind. Eng. Chem. Prod. Res. Dev.* 11 (1972) 393.
- [4] G.L. Bauerle, S.C. Wu and K. Nobe, *Ind. Eng. Chem. Prod. Res. Dev.* 14 (1975) 123.
- [5] K.C. Taylor and R.L. Klimisch, *J. Catal.* 30 (1973) 478.
- [6] K.C. Taylor, R.M. Sinkevitch and R.L. Klimisch, *J. Catal.* 35 (1974) 34.
- [7] R.L. Klimisch and K.C. Taylor, *Ind. Eng. Chem. Prod. Res. Dev.* 14 (1975) 26.
- [8] R.J. Voorhoeve and L.E. Trimble, *J. Catal.* 38 (1975) 80.
- [9] K. Otto and M. Shelef, *Z. Phys. Chem. NF* 85 (1973) 308.
- [10] S.L. Matson and P. Harriot, *Ind. Eng. Chem. Prod. Res. Dev.* 17 (1978) 322.
- [11] M. Uchida and A.T. Bell, *J. Catal.* 60 (1979) 204.
- [12] F. Rosowski, O. Hinrichsen, M. Muhler and G. Ertl, *Catal. Lett.* 36 (1996) 229.
- [13] O. Hinrichsen, F. Rosowski, A. Hornung, M. Muhler and G. Ertl, *J. Catal.* 165 (1997) 33.
- [14] H. Dietrich, K. Jacobi and G. Ertl, *J. Chem. Phys.* 105 (1996) 8944.
- [15] S. Schwegmann, A.P. Seitsonen, H. Dietrich, H. Bludau, H. Over, K. Jacobi and G. Ertl, *Chem. Phys. Lett.* 264 (1997) 680.
- [16] C. Nagl, R. Schuster, S. Renisch and G. Ertl, *Phys. Rev. Lett.* 81 (1998) 3483.
- [17] P.J. Shires, J.R. Cassata, B.G. Mandelik and C.P. van Dijk, *US Patent* 4,479,925 (1984).
- [18] M. Muhler, F. Rosowski, O. Hinrichsen, A. Hornung and G. Ertl, *Stud. Surf. Sci. Catal.* 101 (1996) 317.

- [19] F. Rosowski, A. Hornung, O. Hinrichsen, D. Herein, M. Muhler and G. Ertl, *Appl. Catal. A* 151 (1997) 443.
- [20] R.A. Dalla Betta, *J. Catal.* 34 (1974) 57.
- [21] M. Muhler, F. Rosowski and G. Ertl, *Catal. Lett.* 24 (1994) 317.
- [22] O. Hinrichsen, A. Hornung and M. Muhler, *Chem. Eng. Technol.* 22 (1999) 1039.
- [23] T. Zambelli, J. Wintterlin, J. Trost and G. Ertl, *Science* 273 (1996) 1688.
- [24] R. Burch, P.J. Millington and A.P. Walker, *Appl. Catal. B* 4 (1994) 65.